

Sol gel synthesis and characterization of porous nanosized oxide 70TiO₂-30 MgO film for anode solar cell application

Marwa M. Toraya¹, Doaa M. Atia^{*1}, Amany M. El Nahrawy², Ninet M. Ahmed¹, Saleh Hussin³

¹Photovoltaic Cells Department, Electronics Research Institute (ERI), Cairo, Egypt

²Solid-State Physics Department, Physics Research Division, National Research Centre, 33 El-Bohouth St., Dokki, 12622, Egypt

³Electronics and Communications Engineering Department, Faculty of Engineering, Zagazig University, Egypt

Received 28 November 2021, Revised 22 April 2022, Accepted 13 June 2022

ABSTRACT

This work reports the infusion effect of Mg into TiO₂ nanocomposite for DSSC photo-anode application. TiO₂-MgO Porous nanosized structure oxide film was obtained using sol-gel technique at 400°C. The fabricated film is described in terms of crystallinity and morphology by XRD and HR-SEM. The characterization applied adopted that the fabricated thin-film demonstrated the structure of a semi-crystalline (Ti_{2.94}Mg_{0.06}O₅) and Ti₉O₁₇ nanoparticle. SEM exhibited a smooth surface with crystalline nature predicted to utilize the large efficiency of the solar cells and have matched with the crystallites size that estimated from XRD analysis. The optical spectra showed that porous nanosized 70TiO₂-30MgO film band gap is 2.5 eV. XRD and optical results suggested that the insert of MgO in TiO₂ film compellingly improved the TiO₂ anode thin films.

Keywords: Nanosized Mg-doped TiO₂ thin films; photoanode; DSSC; Sol-gel Method; optical properties

1. INTRODUCTION

In the exploring for alternative, renewable, clean, and economical energy sources, solar cells are a competitive sort of device that yields solar energy and liberate electrical energy. Dye-sensitized solar cells (DSSC) as a type of various solar cells are attractive because of their characteristics such as easy formation, cheaper, and renewability [1]. DSSCs are an outstanding member of the larger group of thin film photovoltaic and DSSC should play a major role in the future of solar energy. DSSCs is one of the third generations of semiconductors-solar cells designed through photo-sensitized electrode (anode), and another one is a counter electrode (cathode) which fabricates a photoelectrochemical arrangement [2]. To yield higher efficiency, some parameters as light absorption and electron injection must be improved. The process of doping certain semiconductors (TiO₂, ZnO, SiO₂, AlO₂, CdO) with a foreign ion to reduce lattice bandgap is very efficient for increasing electron injection [3]. TiO₂ is a semiconductor material used for photo-anode due to its higher transparency, low cost, high availability, high stability, nontoxicity [4]. Because of TiO₂'s excellent optoelectronic, wide band-gap semiconducting materials making TiO₂ one of the most and best choices for different solar energy applications [5]. Nano-TiO₂ as DSSC anode also consider as multi-functional material tenders like air and water purification over the employment of solar energy [6, 7] .

TiO₂ photochemical features worked to convert the solar radiations to efficient energy as in photovoltaic performer and hence encountering a higher deal of consideration. However, solar spectrum utilization has been restricted with a large bandgap of TiO₂ (3.2 eV) [8], most of TiO₂-efficiency can be enhanced through morphological adjustments or by introduction of various non-

* E-mail of corresponding author: doaa@eri.sci.eg

metals and metals components within the TiO₂ framework [9, 10]. The quality of the film and their physical-chemical properties can be improved, the introduction of metal ions is expected to perform a significant part in altering the catalytic activity, the charge carriers contents of the metal oxide ground, the crystallites size, surface potential, phase composition, and so on [11, 12]. Photo activities in photo anode can be improved by doping an alkaline earth metallic material Magnesium Mg into TiO₂ anatase [13]. In addition to enhance the optical properties and preventing the energy migration among TiO₂ ions in TiO₂ anode, it is necessary to introduce some modifies as Mn and Mg centers in the TiO₂ matrix [14]. MgO is considering the finest one in the chains which can modified for the Ti in their bulk because it's ionic radius. Introducing of MgO won't alteration in the crystal assembly. Several methods are approved to form a TiO₂-MgO film such as electrical beam evaporation, Chemical Vapor Deposition (CVD), sputtering, and sol gel. The sol-gel technique has been developed as a widely fabrication method in the last decades by researchers, thus sol-gel technique is adopted here due to several benefits such as the processing can be completed at low temperatures, easy, simple, and cheap. By applying this technique, it is commonly the reactant sols are maintaining nanoparticles in a dispersed state within the applied solvents which successively formed the sol. Further these colloidal particles can be linked together by condensation to get the gel [15][16].

Table 1 presents a list of previous works used TiO₂ as a photoanode in their works. Moreover using various materials as dopants to achieve the photoanode performance and efficiency of the cell are shown. In addition, the methods of fabrication used affected the final performance so it is recommended to focus on it in our work.

Table 1. The relative previous works of TiO₂ photo-anode.

Material Used	Synthesis Method	Reference No.
Sm ³⁺ / Gd ³⁺ doped TiO ₂	Hydrothermal synthesis technique	[17]
Cu/Mn doped TiO ₂	Microwave assisted hydrothermal method	[18]
TiO ₂	Flame spray pyrolysis and hydrothermal Sol-Gel	[19]
Ni/Zn Co-doped TiO ₂	Spin-Coating Technique	[20]
Al doped TiO ₂	Sol-Gel	[21]
Ag doped TiO ₂	Sol-Gel	[22]
MgO doped TiO ₂	Sol-Gel Technique Spin-Coating	[23]

The aim of this study was concentrated on a pure TiO₂ photo-anode in DSSC was replaced by a composite of 70TiO₂-30MgO, this composite was prepared using spin coating sol-gel technology, the prepared composite was deposit on glass substrate, and the deposited thin films were calcinated in air at 400 °C for 1 hr to achieve a porous of 70TiO₂-30MgO layer. The effect of Mg metal on the matrix of TiO₂ has been studied by structural characterization (XRD&SEM) of these films also the optical properties have been studied.

2. EXPERIMENTAL WORK

The preparation and characterization of 70TiO₂-30MgO photo-anode based on spin coating sol-gel method will be described in the following sections. In the following section the materials used,

Note: Accepted manuscripts are articles that have been peer-reviewed and accepted for publication by the Editorial Board. These articles have not yet been copyedited and/or formatted in the journal house style.

the method of preparation is discussed. The characterization of the prepared films using XRD, SEM and UV-VIS-NIR is discussed in details.

2.1 Preparation of 70TiO₂-30MgO Anode.

The 70TiO₂-30MgO thin films were dropped using sol gel spin coating method. The beginning with clean the 2x2 cm², 1.1mm thick glass substrate in ultrasonic by immersing it in acetone followed by washing by distilled water, then the substrates were dried for 5 min at 50°C on hot plate in air before the deposition [5]. The flow chart shown in Fig 1 illustrates that the 70TiO₂-30MgO were synthesized using Titanium Isopropoxide Ti [OCH(CH₃)₂]₄ (TIP), Magnesium nitrate-hexahydrate (Mg(NO₃)₂·6H₂O), which used for thin film deposition without additional purification. At first Magnesium nitrate-hexahydrate dissolved in a mixture of citric acid and distilled water after putting them in magnetic stirring for vigorous stirring. Then, dissolve Titanium Isopropoxide in 15 ml of acetyl acetone and a mixture of a citric acid and distilled water, after that mix the synthesized Titanium Isopropoxide Ti [OCH(CH₃)₂]₄ and Magnesium nitrate-hexahydrate (Mg(NO₃)₂·6H₂O) and making a vigorous stirring for 2 hr in magnetic stirring to obtain Titanium Magnesium solution (TM). The prepared solution is aged for 24 hr in room temperature to obtain the suitable viscosity. The TM solution deposited on glass substrates by using sol-gel - spin coating technique at 1500 rpm for 30 s. The prepared TM thin films will be obtained by drying them using a hot plate at 70 °C in air after each layer deposition to evaporate and remove residual solvents and repeating this step five times to obtain the desired thickness. Finally, the promising 70TiO₂-30MgO thin film calcined at 400 °C for 1 hr. Here the (TM) semiconductors thin film can be ready for all characterization.

2.2 Characterization of 70TiO₂-30MgO Anode Film

The XRD patterns of the promising sensitized (TM) thin film was achieved by Bruker D8 from Germany equipped with CuKα (λ = 1.54 Å) in the 2θ range of 10°–80° and operating at 40 kV and 40 mA. Also, The XRD profile of semi-crystalline film was refined by the profile parameters using Fullprof software (the pseudo-Voigt fitting model) and VESTA-win64 software [24].

The surface morphology of the synthesized 70TiO₂-30MgO thin film was studied using Scanning Electron Microscopy (SEM), Hitachi S4800, Japan, energy dispersive X-ray EDXRF (Shimadzu EDX-7000) . Analysis was performed to determine the concentration of elements and the contaminants in the film. The optical properties of the film were measured using a UV-VIS-NIR spectrophotometer (Shimadzu-2540) in the wavelength range 300-1000nm.

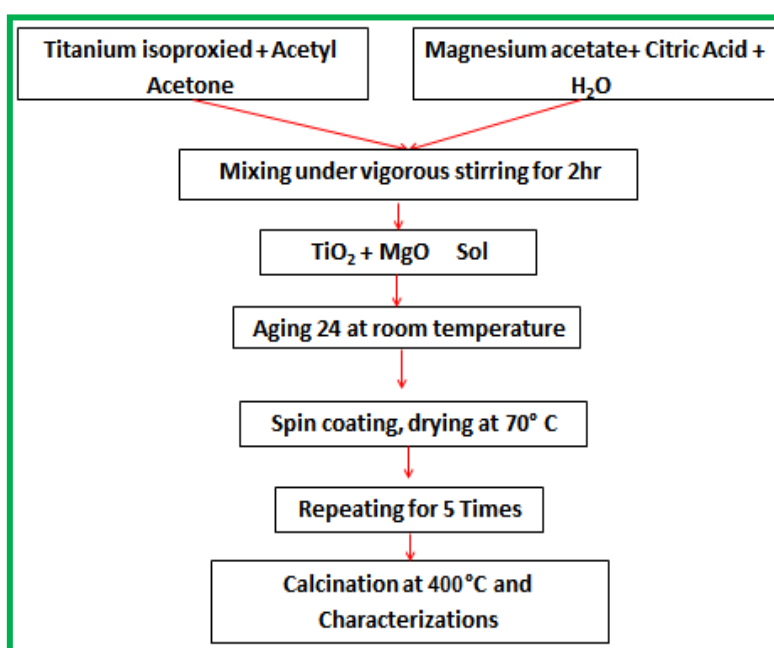


Figure 1 Flow chart of synthesis procedure of 70TiO₂-30 MgO anode film.

3. RESULTS AND DISCUSSIONS

In this section, the structure and optical properties of 70TiO₂-30 MgO anode film will be discussed.

3.1. Structural Evaluation (X-Ray Diffraction)

The X-ray diffraction pattern of porous nanosized 70 TiO₂-30 MgO thin-film obtained by sol-gel method and dropped at glass substrate using spin coating is shown in Fig 2 (a). The obtained XRD show that the deposited film has a semi-crystalline structure and exhibited main peaks at 8.8°, 11.3°, 25.17°, 31.48°, 42°, and 61.62° respectively according to JCPDS card (No. 82-1136) monoclinic magnesium titanate oxide (Mg_{0.06}Ti_{2.9405}) and anorthic titanium oxide (Ti₉O₁₇) card (No. 85-1061) and the main peak at 31.48°.

Generally, the lower intensity of the peaks and the formation of Ti₉O₁₇ phase are formed as a second phase when calcination 70 TiO₂-30 MgO anode film at a lower temperature [25].

It's known that the Mg₂TiO₄ matrix is unstable at low temperatures and may suffer from decomposition to TiO₂ and MgO [26].

Herein, TiO₂-MgO binary nanosized oxide was synthesized by the sol-gel processing [27] caused in a homogeneous sol, through slow rate solvent evaporation leading the gelation occurred at low temperature [28].

A highly porous TiO₂-MgO oxide film with a high surface area was probably owing to the formation of a new magnesium-titanium phase where the nanoparticles can disturb the finest pores of the TiO₂-MgO system.

Scherrer's equation was exercised to calculate the crystallite size; D [29]:

$$D = \frac{(0.9 \lambda)}{(\beta \cos \theta)} \quad (1)$$

Where, θ gives the Bragg's-angle, the full width at half maximum (β) in radians and λ : the X-ray wavelength. The crystallite size (D) of porous nanosized 70 TiO₂-30 MgO thin-film is calculated to be 21 nm at the principle peak (112).

The semi-crystalline structure for TiMg film was confirmed using FullProf-software, as shown in Fig. 2 (b, c). Monoclinic (P 2/c) MgTiO₂ phase was to obtain the Rietveld parameters, where $a=4.51676 \text{ \AA}$, $b=5.50314 \text{ \AA}$, $c=4.88603 \text{ \AA}$, and the cell volume (V) = 121.4429 \AA^3 .

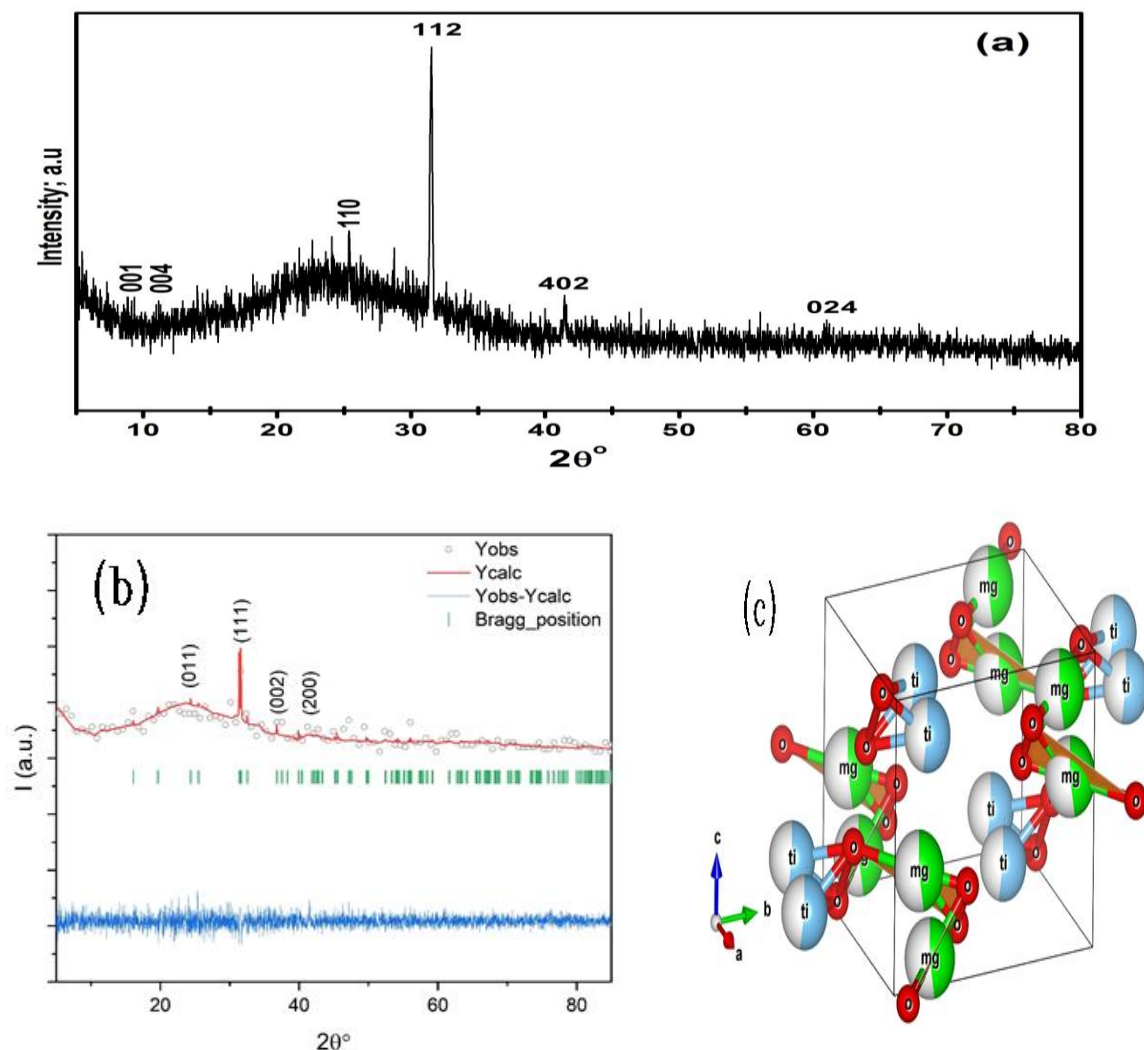


Figure 2 (a) XRD pattern of 70TiO₂-30 MgO anode film, (b) Fullprof XRD pattern and (c) Configuration of 70TiO₂-30 MgO structure

3.2. Films Morphology (SEM/EDX)

The morphology characterization using Scanning Electron Microscopy (SEM) at 20 Kv is illustrated in Fig. 3. The images confirmed the smooth surface for porous nanosized 70TiO₂-30MgO anode film surface synthesized by sol-gel method. Very dense and uniform micrographs of the anode film annealed at 400 °C with an average diameter of 24.9 nm are achieved.

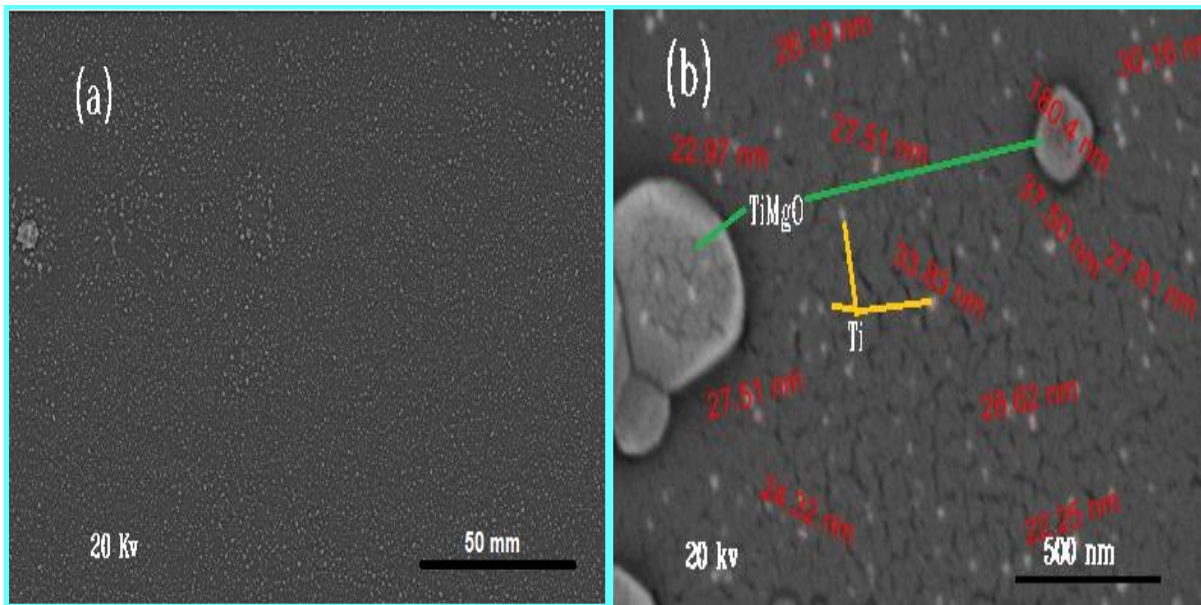


Figure 3 the surface morphology of 70TiO₂-30 MgO anode film.

3.3. Optical properties of oxide 70TiO₂-30 MgO porous nanosized anode film

UV – Vis spectrophotometer is used to scrutinize the optical properties of the synthesized porous nanosized oxide 70TiO₂-30 MgO anode film calcined at 400 °C.

The transmission spectrum for anode thin film in the wavelength range (300- 1000 nm) is shown in Fig.4. The transmittance increases with increasing wavelength (λ) and attains optical transparency over 85% in the visible range. Fig. 5 depicts the reflection spectrum of TM thin film. The reflection reduces with increasing wavelength.

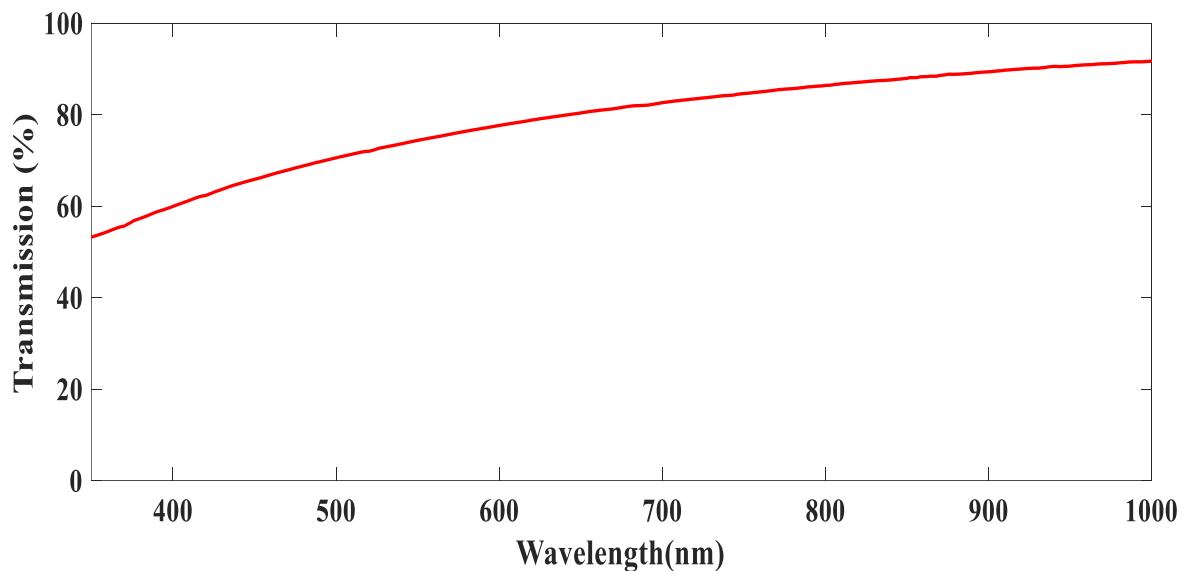


Figure 4 The transmission spectrum of 70TiO₂-30 MgO anode film.

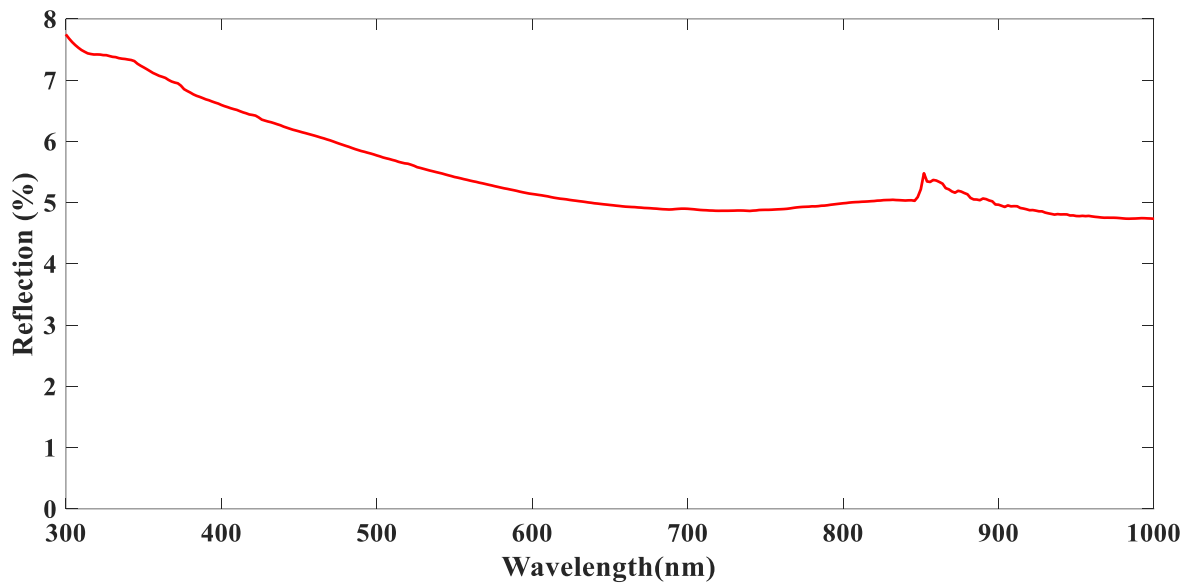


Figure 5 The reflection spectrum of 70TiO₂-30 MgO anode film.

The absorption coefficient deliberated using Lambert law [30], of 70TiO₂-30MgO anode film is shown in Fig. 6.

$$\alpha = \frac{\ln(1/T)}{t} \quad (2)$$

Where 'T' is the transmittance and 't' is the film thickness.

It is observed that the absorption coefficient is high at a lower wavelength and decreases gradually at a higher wavelength. The calculated values of the absorption coefficient are in the order of 10⁴ cm⁻¹.

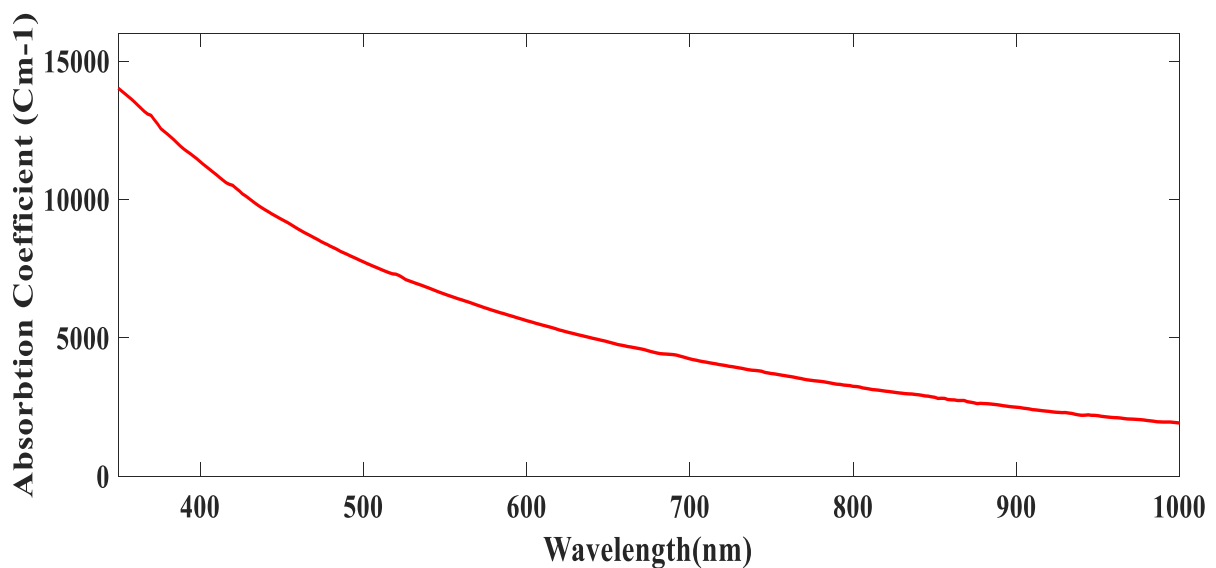


Figure 6 Absorption coefficient of 70TiO₂-30 MgO anode film.

The bandgap of 70TiO₂-30 MgO anode film was estimated using the Tauc relation [31, 32] :

$$(\alpha h\nu)^2 = A(h\nu - E_g) \quad (3)$$

Where α is absorption coefficient, h is Planck's constant, A is constant, ν is frequency of light radiation, E_g is bandgap energy. The bandgap energy was determined via plotting $(\alpha h\nu)^2$ vs. $h\nu$. The value of the bandgap of the film was obtained by extrapolation of the linear region of the plots of $(\alpha h\nu)^2$ to its intersection with the energy axis ($h\nu$). The energy band gap of this sample is 2.5 eV (Fig. 7). It is in good agreement with the value reported elsewhere [33].

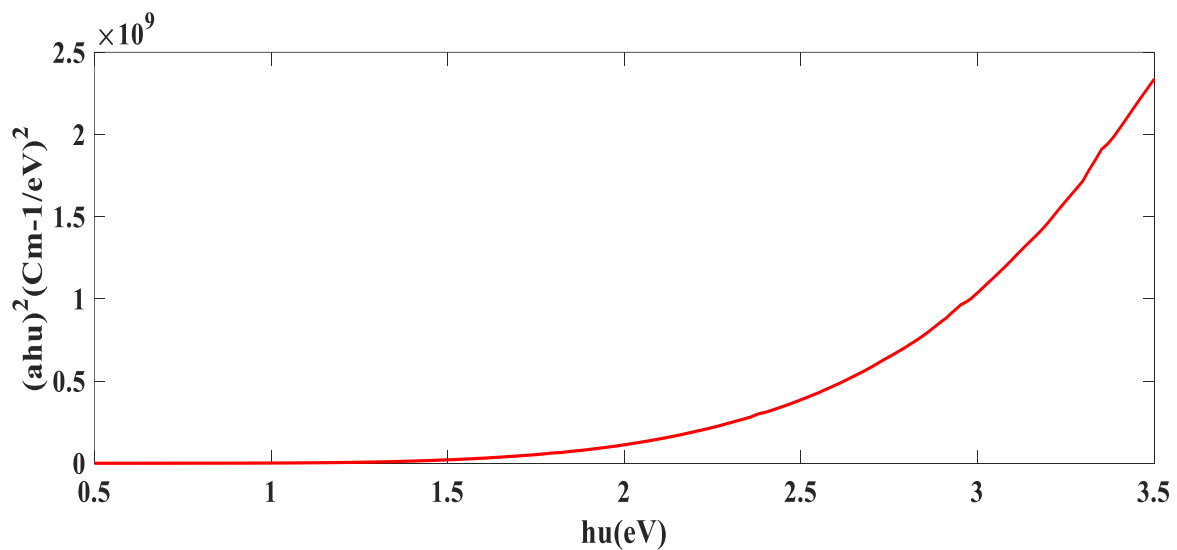


Figure 7 The plots of $(\alpha h\nu)^2$ vs. photon energy of 70TiO₂-30 MgO anode film.

The extinction coefficient (k) of 70TiO₂-30MgO anode film was calculated using the expression:

$$K = \frac{\alpha\lambda}{4\pi} \quad (4)$$

Fig. 8 illustrated the variation of extinction coefficient with wavelength. We perceive that the extinction coefficient drops with an increase in wavelength.

Also, the refractive index (n) of the prepared film can be expressed in terms of the reflection (R) and the extinction coefficients (k) according to the Fresnel equation:

$$n = \frac{1+R}{1-R} + \sqrt{\frac{4R}{(1-R)^2} - K^2} \quad (5)$$

Fig. 9 appeared the decrease in refractive index (n) value of the 70TiO₂-30 MgO thin film with increasing wavelength in normal dispersion region. This conduct might be accredited to various oscillator modes in the semi-crystalline film.

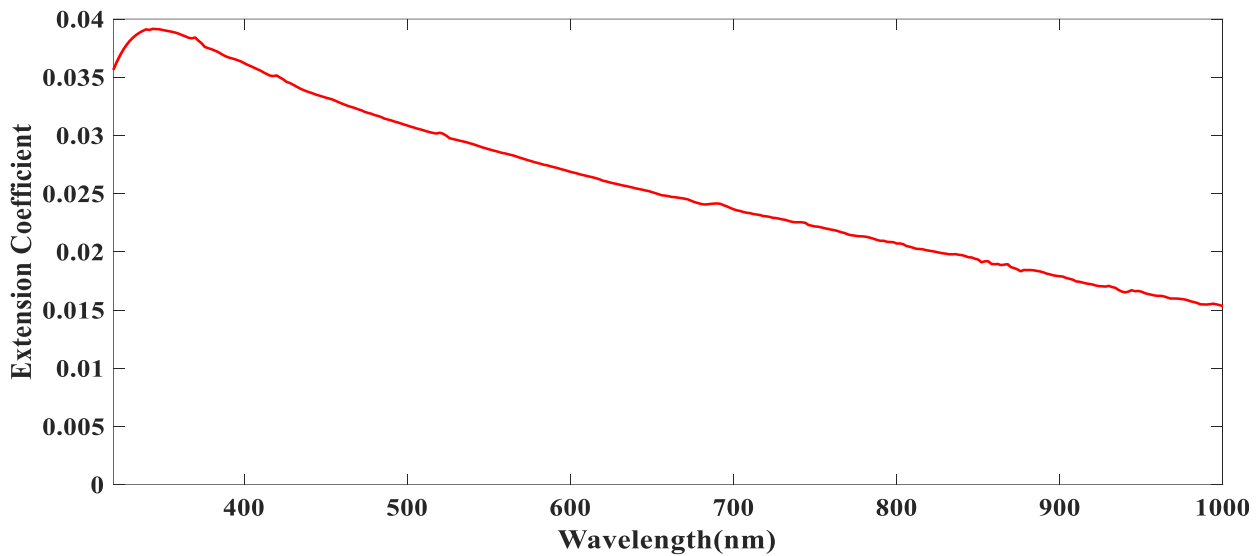


Figure 8 The extinction coefficient variation with wavelength of 70TiO₂-30 MgO anode film.

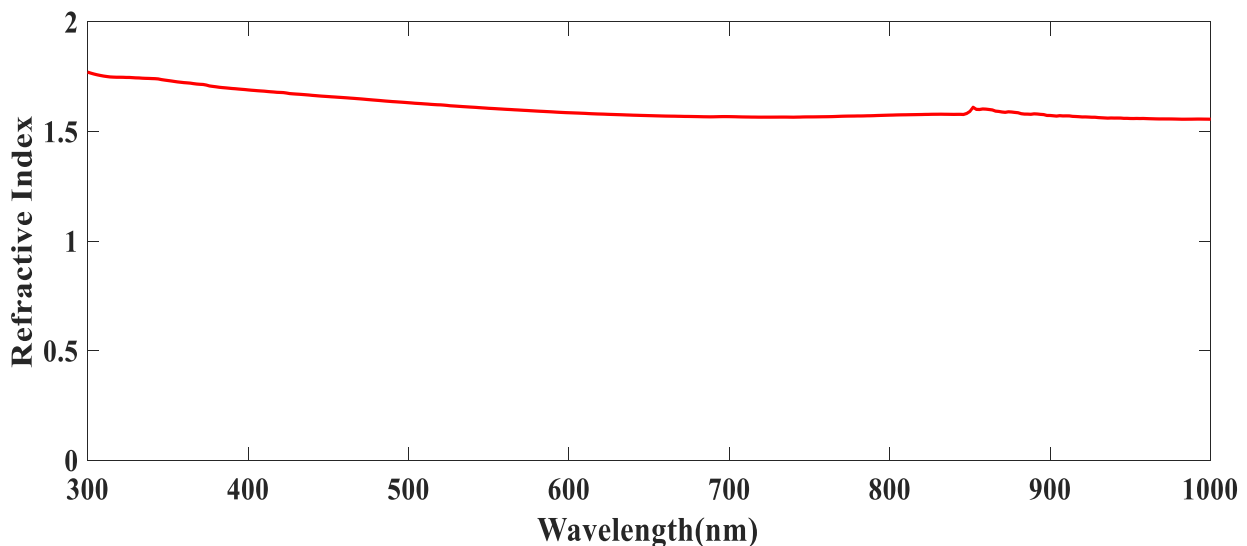


Figure 9 The refractive index variation with wavelength of 70TiO₂-30 MgO anode film.

The estimated dielectric function is an essential intrinsic property and a complex extent of the thin film, which involves both the imaginary parts (ϵ_i) and the real (ϵ_r). The ϵ_r indicates how the rapidity of light in the film can be reduced down however, the imaginary part transactions with the absorption of ($h\nu$) by a dielectric system from the applied electric field owing to the dipole motion.

The estimated dielectric function of the deposited nanosized 70TiO₂-30MgO anode film was intended using the expression:

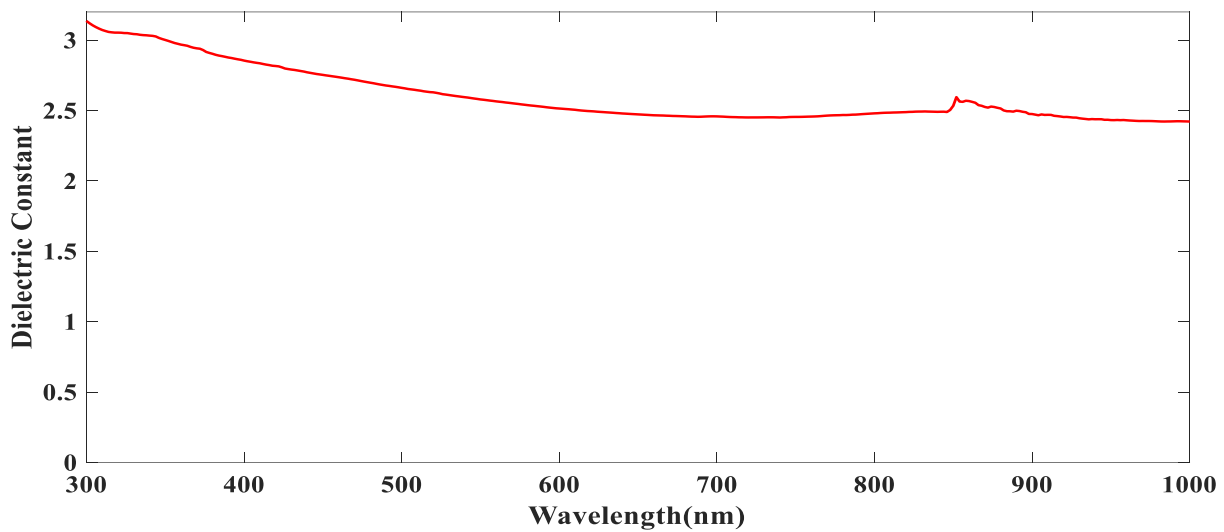
$$\epsilon_T = \epsilon_r + \epsilon_i \quad (6)$$

Real and imaginary fragments of the dielectric constant (ϵ_T) are linked to the (n) and (k) values. The ϵ_r and ϵ_i values were calculated using the formula [34]:

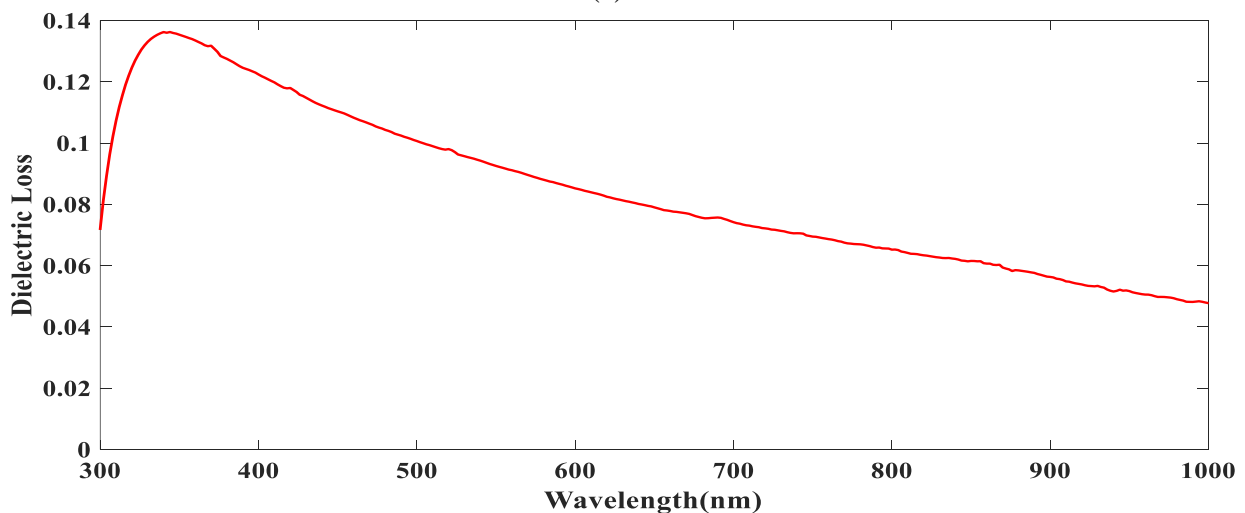
$$\varepsilon_r = n^2 - K^2 \quad (7)$$

$$\varepsilon_i = 2 n K \quad (8)$$

Fig.10 (a, b) illustrates the variation of ε_r (Dielectric Constant) and ε_i (Dielectric Loss) with wavelength. The values of ε_r and ε_i of the nanosized film decrease with incident photon wavelength. The real part of the dielectric constant spectrum is characterized by the presence of the peak at 350 nm may be attributed to a crystalline degree in the film. We see that the behaviour of the real dielectric constant (ε_r) is nearly similar to the refractive index (n) and the behaviour of (ε_i) with photon wavelength is nearly similar to the extinction coefficient and the values of (ε_r) are higher than that of (ε_i).



(a)



(b)

Figure 10 Variation of (a) real and (b) imaginary parts of the dielectric constant of the 70TiO₂-30MgO anode film

The expressions of optical conductivity (σ_{opt}) are mainly concerned with the study of the optical response for any material also, the energy band structure of the deposited film is closely related

to the optical conductivity. The optical conductivity of 70TiO₂-30MgO anode thin film can be calculated by using the absorption coefficient (α) as in the following equation:

$$\sigma_{opt} = \frac{\alpha n c}{4\pi} \quad (9)$$

Where n is the refractive index and c is the velocity of light. Fig. 11 demonstrates the optical conductivity variation as a function of photon wavelength. This behaviour can be attributed to the optical conductivity decreasing with an increase in wavelength also, the absorbance decreasing with an increase in wavelength.

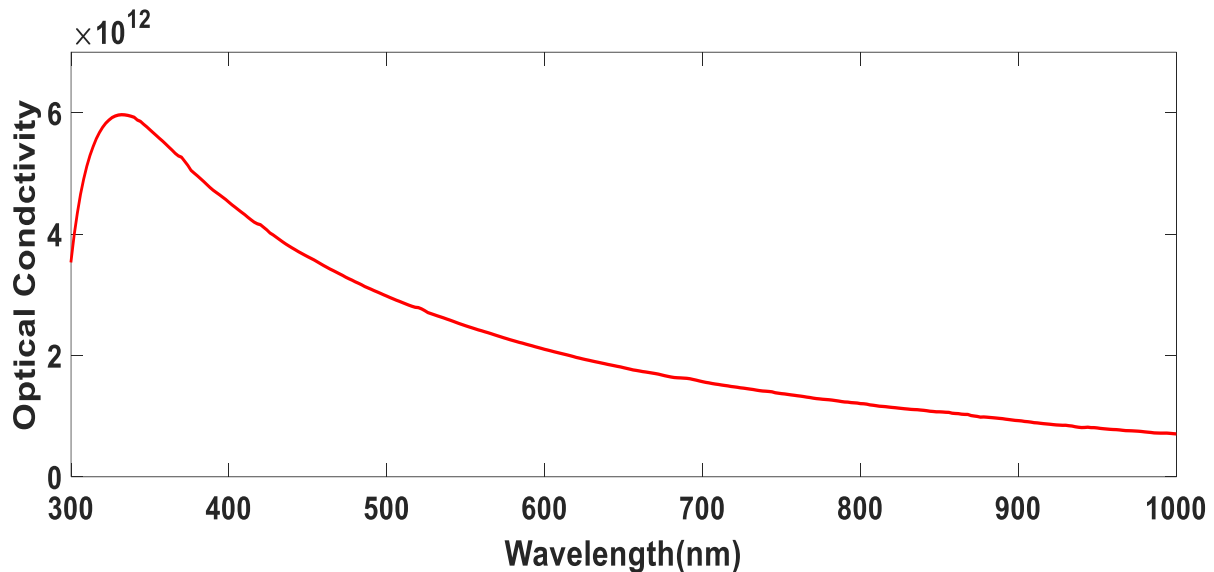


Figure 11 The optical conductivity variation with wavelength of 70TiO₂-30MgO anode film.

The dielectric loss tangent ($\tan \delta$) of 70TiO₂-30MgO thin film, which represents how the electric energy dissipated into thermal energy and can be defined by the following relation:

$$\tan \delta = \frac{\epsilon_i}{\epsilon_r} \quad (10)$$

Where δ is the phase angle between the electric field and the polarization of the dielectric, ϵ_r and ϵ_i are the real and imaginary parts of the dielectric constant, respectively. The dielectric loss tangent of 70TiO₂-30MgO thin film variation with photon wavelength is shown in Fig. 12. It is seen that the loss tangent decreases with increasing the photon wavelength and the change in the $\tan \delta$ is dominated by the variation of ϵ_i .

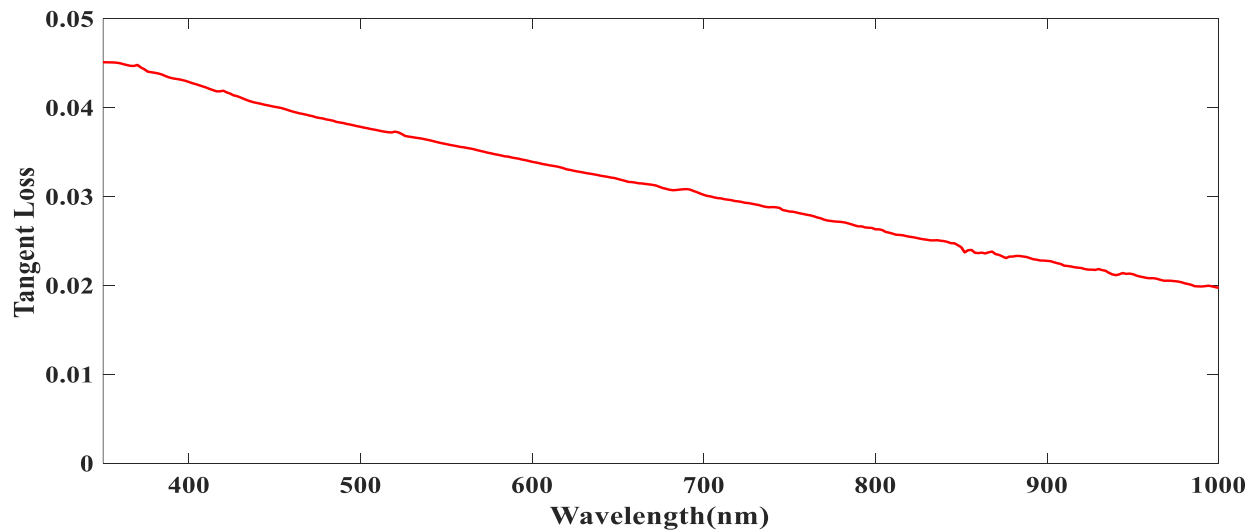


Figure 12. The tangent loss variation with wavelength of 70TiO₂-30MgO anode film

The Q-factor of 70TiO₂-30MgO thin film can be calculated from tangent losses which the quality factor Q is reciprocal of dielectric loss tangent by using the following equation:

$$Q = \frac{1}{\tan\delta} \quad (11)$$

The dependence of quality factor of 70TiO₂-30MgO thin film on photon wavelength is demonstrated in Fig. 13. It is seen that the quality factor of 70TiO₂-30MgO thin film increase with increasing the photon wavelength and this proves that the material with lower ϵ_r generally has a higher Q value.

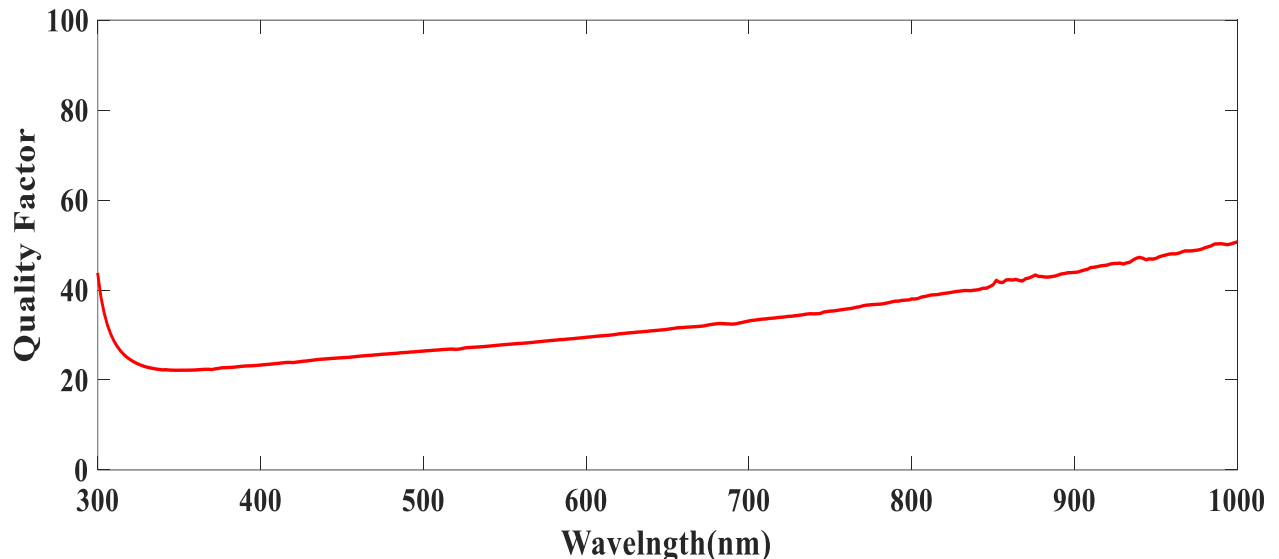


Figure 13. The quality factor variation with a wavelength of 70TiO₂-30MgO anode film.

4. CONCLUSION

70TiO₂-30MgO thin film was magnificently prepared by the sol-gel method. Structural and optical properties of the prepared porous nanosized thin films were investigated. The transmittance of the synthesized films exceeded 85 % in the visible range. The bandgap for 70TiO₂-30MgO was estimated to be 2.5 eV, which is in good agreement with the reported value in the literature. The accidental distribution of the formed grains makes the film surface irregular and increased the light scattering sufferers at the interface. Illustrated low bandgap, high absorption may be suitable for different photovoltaic applications. Studying alternative dopants and dopant percentages effect on the TiO₂ properties will be considered in future.

References

- [1] Y. . W. J. Wu, Z. Lan, J. Lin, M. Huang, Y. Huang, L. Fan, G. Luo, Y. Lin, Y. Xie, "Counter electrodes in dye-sensitized solar cells," *Chem. Soc. Rev.*, pp. 5975–6023, 2017, doi: 10.1039/c6cs00752j.
- [2] S. Sathyajothi, R. Jayavel, and A. C. Dhanmozhi, "The Fabrication of Natural Dye Sensitized Solar Cell (Dssc) based on TiO₂ Using Henna And Beetroot Dye Extracts," *Mater. Today Proc.*, vol. 4, no. 2, pp. 668–676, 2017, doi: 10.1016/j.matpr.2017.01.071.
- [3] M. Safaei, "The International Debate on Preparation of Mg-Doped TiO₂ Nanoparticles for Dye-Sensitized Solar Cell Applications," *J. Clin. Pathol. Lab. Med.*, vol. 1, 2020.
- [4] W. Rho, D. H. Song, H. Yang, H. Kim, and B. S. Son, "Recent advances in plasmonic dye-sensitized solar cells," *J. Solid State Chem.*, vol. 258, no. October 2017, pp. 271–282, 2018, doi: 10.1016/j.jssc.2017.10.018.
- [5] S. Shakir, M. Abd-ur-Rehman, K. Yunus, and M. Iwamoto, "Fabrication of un-doped and magnesium doped TiO₂ films by aerosol assisted chemical vapor deposition for dye sensitized solar cells," *J. Alloy. Compd. J.*, vol. 737, pp. 740–747, 2018, doi: 10.1016/j.jallcom.2017.12.165.
- [6] A. J. Maira, K. L. Yeung, C. Y. Lee, P. L. Yue, and C. K. Chan, "Size Effects in Gas-Phase Photo-oxidation of Trichloroethylene Using Nanometer-Sized TiO₂ Catalysts," vol. 196, pp. 185–196, 2000, doi: 10.1006/jcat.2000.2838.
- [7] L. Lu, X. Xia, J. K. Luo, and G. Shao, "Mn-doped TiO₂ thin films with significantly improved optical and electrical properties," vol. 485102, doi: 10.1088/0022-3727/45/48/485102.
- [8] A. V Emeline, V. N. Kuznetsov, V. K. Rybchuk, and N. Serpone, "Visible-Light-Active Titania Photocatalysts : The Case of N-Doped TiO₂s — Properties and Some Fundamental Issues," vol. 2008, 2008, doi: 10.1155/2008/258394.
- [9] T. Umabayashi, T. Yamaki, H. Itoh, and K. Asai, "Band gap narrowing of titanium dioxide by sulfur doping," vol. 454, no. 2002, pp. 3–6, 2012, doi: 10.1063/1.1493647.
- [10] M. Devi and M. R. Panigrahi, "Effect of annealing temperature on the optical and electrical properties of Mg doped TiO₂ thin films," vol. 10, pp. 63–74, 2017.
- [11] J. Gong, J. Liang, and K. Sumathy, "Review on dye-sensitized solar cells (DSSCs): Fundamental concepts and novel materials," *Renew. Sustain. Energy Rev.*, vol. 16, no. 8, pp. 5848–5860, 2012, doi: 10.1016/j.rser.2012.04.044.
- [12] D. Szczuko, J. Werner, S. Oswald, G. Behr, and K. Wetzig, "XPS investigations of surface segregation of doping elements in SnO₂," vol. 179, pp. 1–6, 2001.
- [13] Y. Sui *et al.*, "Investigation of Optimum Mg Doping Content and Annealing Parameters of Cu₂MgxZn_{1-x}SnS₄ Thin Films for Solar Cells," *nanomaterials*, vol. 9, pp. 1–13, 2019, doi: 10.3390/nano9070955.
- [14] C. Vigreux, B. Deneuve, J. El Fallah, and J. M. Haussonne, "Effects of acceptor and donor additives on the properties of MgTiO₃ ceramics sintered under reducing atmosphere," vol. 21, pp. 1681–1684, 2001.
- [15] V. Yuniar and E. Yufita, "Structural and optical properties of MgO- doped TiO₂ prepared by sol-gel method Structural and Optical Properties of MgO-doped TiO₂ Prepared by Sol-Gel Method," vol. 110007, no. March, 2020.
- [16] U. Singh, L. Bhattacharyya, S. Kumar, R. Mishra, G. Sharma and S. Singh, G. Ahalawat, "Sol-Gel processing of silica nanoparticles and their applications," *Adv. Colloid Interface Sci.*, vol. 214, pp. 17–37, 2014, doi: 10.1016/j.cis.2014.10.007.
- [17] M. R. S. Bernadsha, V. Samson, N. Simi, J. Madhavan, "Analyzing the efficiency of nanostructured Sm³⁺ and Gd³⁺ doped TiO₂ and constructing DSSCs using efficacious photoanodes," *J. Mater. Sci. Mater. Electron.*, vol. 33, no. 9, pp. 6446–6455, 2022, doi: 10.1007/s10854-022-07816-7.

- [18] B. Ünlü and M. Özacar, "Effect of Cu and Mn amounts doped to TiO₂ on the performance of DSSCs," *Sol. Energy*, vol. 196, pp. 448–456, Jan. 2020, doi: 10.1016/j.solener.2019.12.043.
- [19] A. Aboulouard *et al.*, "Dye sensitized solar cells based on titanium dioxide nanoparticles synthesized by flame spray pyrolysis and hydrothermal sol-gel methods: A comparative study on photovoltaic performances," *J. Mater. Res. Technol.*, vol. 9, no. 2, pp. 1569–1577, 2020, doi: 10.1016/j.jmrt.2019.11.083.
- [20] T. S. Bramhankar *et al.*, "Effect of Nickel-Zinc Co-doped TiO₂ blocking layer on performance of DSSCs," *J. Alloys Compd.*, vol. 817, p. 152810, Mar. 2020, doi: 10.1016/j.jallcom.2019.152810.
- [21] M. Geetha *et al.*, "Preparation and characterisation of tailored TiO₂ nanoparticles photoanode for dye sensitised solar cells To cite this version : HAL Id : hal-03108287 I NTERNATIONAL J OURNAL OF Preparation and Characterisation of Tailored TiO₂ nanoparticles Photoanode f," 2021.
- [22] A. K. Gupta, P. Srivastava, and L. Bahadur, "Improved performance of Ag-doped TiO₂ synthesized by modified sol-gel method as photoanode of dye-sensitized solar cell," *Appl. Phys. A Mater. Sci. Process.*, vol. 122, no. 8, pp. 1–13, 2016, doi: 10.1007/s00339-016-0241-2.
- [23] A. Merazga, F. Al-Subai, A. M. Albaradi, A. Badawi, A. Y. Jaber, and A. A. B. Alghamdi, "Effect of sol-gel MgO spin-coating on the performance of TiO₂-based dye-sensitized solar cells," *Mater. Sci. Semicond. Process.*, vol. 41, pp. 114–120, Jan. 2016, doi: 10.1016/j.mssp.2015.08.026.
- [24] K. Momma and F. Izumi, "VESTA : a three-dimensional visualization system for electronic and structural analysis," pp. 653–658, 2008, doi: 10.1107/S0021889808012016.
- [25] K. Sreedhar and N. Pavaskar, "Synthesis of MgTiO₃ and Mg₄Nb₂O₉ using stoichiometrically excess MgO," *Mater. Lett.*, vol. 53, pp. 452–455, 2002, doi: doi.org/10.1016/S0167-577X(01)00525-0.
- [26] L. Borkovska *et al.*, "Optical and structural properties of Mn-doped magnesium titanates fabricated with excess MgO," *Mater. Today Commun.*, vol. 27, 2021, doi: 10.1016/j.mtcomm.2021.102373.
- [27] A. A. Elabd, O. A. Elhefnawy, and A. M. El Nahrawy, "RSC Advances A new organic-silica based nanocomposite prepared for spectrophotometric determination of uranyl ions," *RSC Adv.*, vol. 6, pp. 9563–9570, 2016, doi: 10.1039/C5RA21401G.
- [28] A. A. Haroun, A. M. El Nahrawy, and P. Maincent, "based nanogels for sustained drug delivery systems," vol. 86, no. 5, pp. 691–700, 2014, doi: 10.1515/pac-2013-1110.
- [29] A. El Nahrawy, A. Bakr, B. Hemdan, and A. A. Hammad, "Identification of - Fe³⁺ co-doped zinc titanate mesostructures using dielectric and antimicrobial activities," *Int. J. Environ. Sci. Technol.*, no. 0123456789, 2020, doi: 10.1007/s13762-020-02786-x.
- [30] A. El Nahrawy, A. Abou Hammad, and A. Mansour, "Compositional Effects and Optical Properties of P2O₅ Doped Magnesium Silicate Mesoporous Thin Films," *Arab. J. Sci. Eng.*, 2020, doi: 10.1007/s13369-020-05067-4.
- [31] A. El-Nahrawy, A. Ali, A. Abou Hammad, A. Youssef, "Influences of Ag-NPs doping chitosan/calcium silicate nanocomposites for optical and antibacterial activity," *Int. J. Biol. Macromol.*, 2016, doi: 10.1016/j.ijbiomac.2016.08.045.
- [32] Y. Caglar, M. Caglar, and S. Ilican, "Microstructural , optical and electrical studies on sol gel derived ZnO and ZnO : Al fi lms," *Curr. Appl. Phys.*, vol. 12, no. 3, pp. 963–968, 2012, doi: 10.1016/j.cap.2011.12.017.
- [33] M. N. An, S. Radiman, N. M. Huang, and M. A. Yarmo, "Sol - gel hydrothermal synthesis of bismuth - TiO₂ nanocubes for dye-sensitized solar cell," vol. 36, pp. 2215–2220, 2010, doi: 10.1016/j.ceramint.2010.05.027.
- [34] A. Mansour, A. Abou Hammad, and A. El Nahrawy, "Nano-Structures & Nano-Objects Sol - gel synthesis and physical characterization of novel photodiode," *Nano-Structures & Nano-Objects*, vol. 25, p. 100646, 2021, doi: 10.1016/j.nanoso.2020.100646.